

SDDBENCH: A BENCHMARK FOR SYNTHESIZABLE DRUG DESIGN

Anonymous authors

Paper under double-blind review

ABSTRACT

A significant challenge in wet lab experiments with current drug design generative models is the trade-off between pharmacological properties and synthesizability. Molecules predicted to have highly desirable properties are often difficult to synthesize, while those that are easily synthesizable tend to exhibit less favorable properties. As a result, evaluating the synthesizability of molecules in general drug design scenarios remains a significant challenge in the field of drug discovery. The commonly used synthetic accessibility (SA) score aims to evaluate the ease of synthesizing generated molecules, but it falls short of guaranteeing that synthetic routes can actually be found. Inspired by recent advances in top-down synthetic route generation and forward reaction prediction, we propose a new, data-driven metric to evaluate molecule synthesizability. This novel metric leverages the synergistic duality between retrosynthetic planners and reaction predictors, both of which are trained on extensive reaction datasets. To demonstrate the efficacy of our metric, we conduct a comprehensive evaluation of round-trip scores across a range of representative molecule generative models.

1 INTRODUCTION

Drug design is a fundamental problem in machine learning for drug discovery. However, when these computationally predicted molecules are put to the test in wet lab experiments, a critical issue often arises: many of them prove to be unsynthesizable in practice (Parrot et al., 2023). This synthesis gap can be attributed to two primary factors. Firstly, while structurally feasible, the predicted molecules often lie far beyond the known synthetically-accessible chemical space (Ertl & Schuffenhauer, 2009). This significant departure from known chemical territory makes it extremely difficult, and often impossible, to discover feasible synthetic routes (Segler et al., 2018; Liu et al., 2023b). This synthesis challenge is underscored by numerous clinical drugs derived from natural products, which, due to their intricate structures, can only be obtained through direct extraction from natural sources rather than synthesis methods (Zheng et al., 2022). These natural products often have complex ring structures and multiple chiral centers, which makes their chemical synthesis challenging (Paterson & Anderson, 2005). Additionally, the biological processes that create these compounds are frequently not well understood, increasing the complexity of laboratory synthesis. Secondly, even when plausible reactions are identified based on literature, they may fail in practice due to the inherent complexity of chemistry (Lipinski, 2004). The sensitivity of chemical reactions is such that even minor changes in functional groups can potentially prevent a reaction from happening as anticipated.

The ability to synthesize designed molecules on a large scale is crucial for drug development. Some current methods (You et al., 2018; Gao & Coley, 2020) rely on the Synthetic Accessibility (SA) score (Ertl & Schuffenhauer, 2009) for synthesizability evaluation. This score assesses how easily a drug can be synthesized by combining fragment contributions with a complexity penalty. However, this metric has limitations as it evaluates synthesizability based on structural features and fails to account for the practical challenges involved in developing actual synthetic routes for these molecules. In other words, a high SA score does not guarantee that a feasible synthetic route for the molecule can be identified using available molecule synthesis tools (Genheden et al., 2020; Tripp et al., 2022).

To overcome the limitations of the SA score, recent works (Cretu et al., 2024) have employed retrosynthetic planners or AiZynthFinder (Genheden et al., 2020) to evaluate the synthesizability of generated molecules. These tools are used to find synthetic routes and assess the proportion of

054 molecules for which routes can be found. As a result, these works rely on the search success rate
055 for evaluating molecule synthesizability. However, this metric is overly lenient, as it fails to ensure
056 that the proposed routes are actually capable of synthesizing the target molecules (Liu et al., 2023b).
057 In practice, many reactions predicted by these tools may not be simulated in the wet lab, as these
058 tools often rely on data-driven retrosynthesis models prone to predicting unrealistic or hallucinated
059 reactions Zhong et al. (2023); Tripp et al. (2024).

060 To address the overly lenient evaluation metrics in previous retrosynthesis studies, where success
061 is often defined merely by finding a “solution” without any regard to whether the solution can be
062 executed in the wet lab (Tripp et al., 2024), FusionRetro (Liu et al., 2023b) proposes assessing
063 whether the starting materials¹ of a predicted route of a target molecule match those in reference
064 routes from the literature database for a target molecule. However, for new molecules generated by
065 drug design models, reference synthetic routes are often unavailable in literature databases. This
066 raises a critical question:

067 *Can data-driven retrosynthetic planners be used to evaluate the synthesizability of these molecules?*

068 Inspired by recent advancements that leverage forward reaction models (Sun et al., 2021) to en-
069 hance retrosynthesis algorithms and rank the top-k synthetic routes predicted by retrosynthetic
070 planners (Schwaller et al., 2019b; Liu et al., 2024a), we propose a three-stage approach that incorpo-
071 rates forward reaction models for evaluating molecule synthesizability to address this question.

072 Our evaluation process consists of three stages. In the first stage, we use a retrosynthetic planner to
073 predict synthetic routes for molecules generated by drug design generative models. In the second
074 stage, we assess the feasibility of these routes using a reaction prediction model as a simulation
075 agent, serving as a substitute for wet lab experiments. This model attempts to reconstruct both the
076 synthetic route and the generated molecule, starting from the predicted route’s starting materials. In
077 the third stage, we calculate the Tanimoto similarity, also called the round-trip score, between the
078 reproduced molecule and the originally generated molecule as the synthesizability evaluation metric.
079 Our proposed metric also draws inspiration from evaluation methods used in image generation, such
080 as the CLIP score (Radford et al., 2021; Hessel et al., 2021). In image generation, the CLIP score
081 assesses the similarity between generated images and their corresponding text descriptions using
082 the pre-trained CLIP model (Radford et al., 2021). Analogously, our point-wise round-trip score
083 evaluates whether the starting materials in a predicted synthetic route can successfully undergo a
084 series of reactions to produce the generated molecule.

085 With the round-trip score as the foundation, we develop a new benchmark to evaluate the “synthesiz-
086 ability” of molecules predicted by current structure-based drug design (SBDD) generative models.
087 Our contributions can be summarized as follows:

- 088 • We recognize the limitations of the current metrics used for evaluating molecule synthesizability.
089 Therefore, we propose the round-trip score as a metric to evaluate the synthesizability of new
090 molecules generated by drug design models.
- 091 • We develop a new benchmark based on the round-trip score to evaluate existing generative models’
092 ability to predict synthesizable drugs. This benchmark aims to shift the focus of the entire research
093 community towards synthesizable drug design.

094 095 096 2 BACKGROUND

097 In this section, we discuss the details of drug design and molecule synthesis. Machine learning algo-
098 rithms for molecule synthesis can be categorized into three main types: forward reaction prediction
099 models, backward retrosynthesis prediction models, and search algorithms.

100 101 102 2.1 STRUCTURE-BASED DRUG DESIGN

103 While our newly developed benchmark is capable of evaluating a wide range of drug design mod-
104 els, this work specifically focuses on assessing the synthesizability of molecules generated by
105

106 ¹Starting materials are defined as commercially purchasable molecules. ZINC (Sterling & Irwin, 2015)
107 provides open-source databases of purchasable compounds, and we define the compounds listed in these
databases as our starting materials.

SBDD models. The primary goal of SBDD is to generate ligand molecules capable of binding to a specific protein binding site. In this context, we represent the target protein and ligand molecule as $\mathbf{p} = \{(\mathbf{x}_i^p, \mathbf{v}_i^p)\}_{i=1}^{N_p}$ and $\mathbf{m} = \{(\mathbf{x}_i^m, \mathbf{v}_i^m)\}_{i=1}^{N_m}$, respectively. Here, N_p and N_m denote the number of atoms in the protein \mathbf{p} and ligand \mathbf{m} . For each atom, $\mathbf{x} \in \mathbb{R}^3$ represents its position in three-dimensional space, while $\mathbf{v} \in \mathbb{R}^K$ encodes its type. The core challenge of SBDD lies in accurately modeling the conditional distribution $P(\mathbf{m} \mid \mathbf{p})$.

2.2 REACTION PREDICTION

Reaction prediction aims to determine the outcome of a chemical reaction. The task involves predicting the products $\mathcal{M}_p = \{m_p^{(i)}\}_{i=1}^n \subseteq \mathcal{M}$ given a set of reactants $\mathcal{M}_r = \{m_r^{(i)}\}_{i=1}^m \subseteq \mathcal{M}$, where \mathcal{M} represents the space of all possible molecules. It’s worth noting that in current public reaction datasets, such as USPTO (Lowe, 2014), only the main product is typically recorded (i.e., $n = 1$), with by-products often omitted. This simplification, while practical for many applications, has a limitation in capturing the full complexity of chemical reactions.

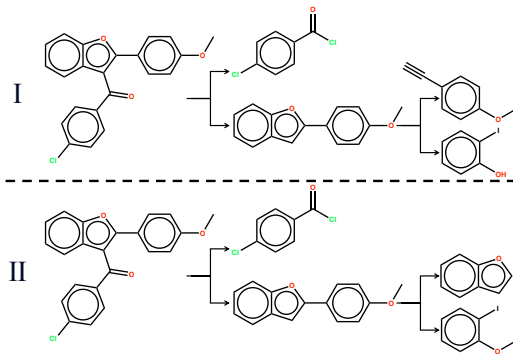


Figure 1: For a given molecule, multiple synthetic routes can be identified within the reaction database, illustrating the diverse routes available for its synthesis.

2.3 RETROSYNTHESIS PREDICTION

Retrosynthesis, the inverse process of reaction prediction, aims to identify a set of reactants $\mathcal{M}_r = \{m_r^{(i)}\}_{i=1}^m \subseteq \mathcal{M}$ capable of synthesizing a given product molecule m_p through a single chemical reaction. This process essentially works backward from the desired product, determining the precursor molecules necessary for its synthesis. By doing so, retrosynthesis plays a crucial role in planning synthetic routes for complex molecules, particularly in drug discovery and materials science.

2.4 REACTION PREDICTION (FORWARD) VS. RETROSYNTHESIS PREDICTION (BACKWARD)

Reaction prediction and retrosynthesis prediction differ fundamentally in their nature and objectives. Reaction prediction is a deterministic task, where specific reactants under given conditions typically yield a predictable outcome. In contrast, retrosynthesis prediction is inherently a one-to-many task, providing multiple potential routes to a desired product as illustrated in Figure 1.

2.5 RETROSYNTHETIC PLANNING

Retrosynthetic planning is a strategic approach to predict synthetic routes for target molecules. This process works backward from the desired target, identifying potential precursor molecules that could be transformed into the target through chemical reactions. These precursors are then further decomposed into simpler, readily available starting materials or building blocks. A synthetic route can be formally represented as a tuple with four elements: $\mathcal{T} = (m_{tar}, \tau, \mathcal{I}, \mathcal{B})$, where $m_{tar} \in \mathcal{M} \setminus \mathcal{S}$ is the target molecule, $\mathcal{S} \subseteq \mathcal{M}$ represents the space of starting materials, $\mathcal{B} \subseteq \mathcal{S}$ denotes the specific starting materials used, τ is the series of reactions leading to m_{tar} , and $\mathcal{I} \subseteq \mathcal{M} \setminus \mathcal{S}$ represents the intermediates. In organic synthesis, a “route” refers to the complete flowchart of reactions required to synthesize a target molecule, as illustrated in Figure 1. This definition differs from its usage in computer science. Synthetic routes can be classified as convergent (Figure 1) or non-convergent, depending on whether the reactions within the route have branching points (Gao et al., 2022a). The planning process is iterative. At each step, single-step retrosynthesis models predict various sets of potential reactants that could lead to the desired product. A search algorithm then selects the most promising solutions to extend the synthetic route further. This process continues until all leaf nodes correspond to readily available starting materials, resulting in a complete synthetic route from purchasable molecules to the target compound.

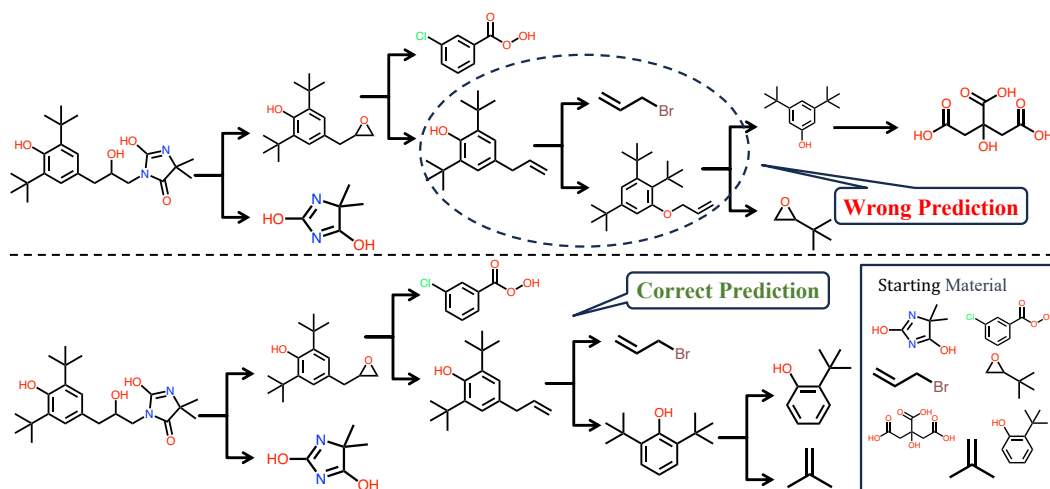


Figure 2: Comparison of evaluation metrics for retrosynthetic planning. The search success rate deems both routes successful, while the matching-based metric correctly identifies the top route as incorrect and the bottom route as correct, demonstrating its superior reliability.

2.6 EVALUATION OF MOLECULE SYNTHESIS

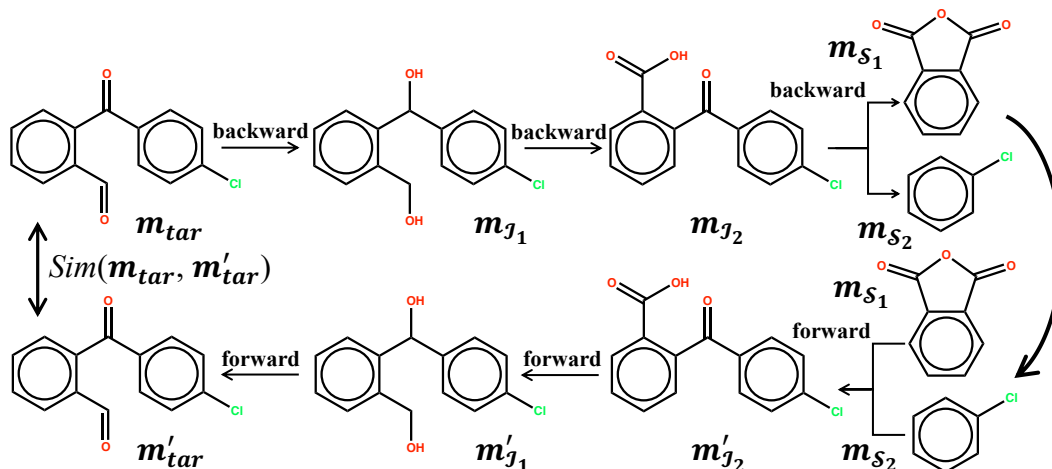
Current evaluation methods for single-step reaction and retrosynthesis predictions primarily rely on the exact match metric. This approach assesses whether the predicted results match the ground truth in the test dataset. Typically, multiple predictions are generated, and the top-k test accuracy is reported.

Until recently, evaluation criteria for retrosynthetic planning had not reached a clear consensus, but they have now converged on a few key metrics. Among these, one of the most widely used is the success rate of finding a synthetic route within a limited number of calls for single-step retrosynthesis prediction (typically capped at 500). However, this metric, known as the search success rate, is overly lenient as it does not verify whether the searched synthetic route can be executed in the wet lab to synthesize the target molecule. This limitation is particularly problematic for targets requiring long synthetic routes, where errors can accumulate across multiple steps.

To illustrate this limitation, we observe that existing single-step models achieve top-5 accuracies of less than 80% (Somnath et al., 2021). In contrast, current retrosynthetic planning methods report search success rates exceeding 99% (Xie et al., 2022) under the limit of 500 single-step retrosynthesis prediction iterations. This discrepancy is counterintuitive since longer synthetic routes should inherently have a lower likelihood of success due to the increasing complexity of the synthesis. This raises concerns about the quality of the routes deemed “successful” by multi-step planners.

To address the limitations of using search success rate as an evaluation metric for retrosynthetic planning, FusionRetro (Liu et al., 2023b) introduces a matching-based evaluation approach. This method compares the starting materials of synthetic routes predicted by retrosynthetic planners for target molecules with those from reference routes retrieved from literature databases. If the starting materials of a predicted route match those of any reference route, the prediction is considered accurate and successful. This approach aligns with the evaluation methodology used in single-step retrosynthesis, which also relies on literature databases. Moreover, FusionRetro goes further by constructing a reaction network from all reactions in the literature database. For a given target molecule, it extracts all synthetic routes from this reaction network, with the leaf nodes within these routes being the starting materials. As FusionRetro reports, this often enables the identification of multiple synthetic routes for a target molecule within the literature database.

While this matching-based approach has its limitations such as the inability of current literature databases to cover all equivalent synthetic routes to a target molecule, this limitation is not unique to FusionRetro and also applies to existing retrosynthesis evaluation methods. Despite this, the



233 Figure 3: Illustration of the round-trip score calculation process. It consists three stages: Retrosyn-
234 thetic Planning, Forward Reproduction, and Similarity Computation.

237 matching-based evaluation metric is a more reliable and rigorous alternative to the search success
238 rate.

239 To illustrate the differences between the two metrics, we introduce an example in Figure 2. The
240 top part of the figure shows a predicted synthetic route where the retrosynthesis prediction within
241 the highlighted circle is incorrect, while the bottom part illustrates a correctly predicted synthetic
242 route. Despite this, both routes are considered successful under the search success rate metric. This is
243 because the search success rate evaluates the solvability of finding a route with leaf nodes as starting
244 materials within a limited number of single-step retrosynthesis prediction iterations for a given target
245 molecule.

246 In contrast, the starting material matching-based metric clearly distinguishes between the two routes.
247 It identifies the top route as incorrect and the bottom route as correct, as the incorrect route in
248 the top example would not match any entries in the literature reaction database. This example
249 intuitively demonstrates that the matching-based evaluation metric provides a more reliable and
250 accurate assessment than the search success rate.

252 3 ROUND-TRIP SCORE

255 In this section, we introduce a novel metric called the round-trip score. This metric is designed to
256 assess the feasibility of synthetic routes for molecules generated by drug design models. Specifically, it
257 evaluates the probability that retrosynthetic planners, trained on current reaction data, can successfully
258 predict feasible synthetic routes for these proposed molecules.

260 3.1 MOTIVATION

262 As discussed in Sections 1 and 2, current heuristics-based metrics for evaluating molecule synthe-
263 sizability, such as the SA score, fail to ensure that synthetic routes can be identified using existing
264 data-driven molecule synthesis tools. However, these tools typically rely on the search success rate as
265 a metric, which does not assess the feasibility of the predicted routes. We have identified a critical
266 flaw in the search success rate metric in Section 2.6 and find that the match-based evaluation metric
267 provides a more reliable alternative.

268 However, for new molecules generated by drug design generative models, reference routes are often
269 missing from literature databases, making it impossible to evaluate predicted routes using match-
based metrics. Ideally, the most accurate evaluation would involve directly validating the predicted

270 routes in the wet lab to confirm whether they can synthesize the target molecules. However, this
271 approach is prohibitively expensive, especially when evaluating large numbers of molecules.

272 To address this challenge, we note that recent forward reaction prediction models achieve top-1
273 accuracies exceeding 90% (Bi et al., 2021). These models can simulate reactions to verify whether
274 the predicted synthetic routes are capable of synthesizing the target molecules. While this approach
275 has its limitations, it is far more reliable than the search success rate and avoids the significant costs
276 associated with wet lab experiments.

277 278 3.2 THREE-STAGE EVALUATION PROCESS

279 In this section, we discuss the details of three stages of our evaluation method: retrosynthetic planning,
280 forward reaction prediction, and similarity computation.

281 Given a molecule m proposed by a generative model, we first use a retrosynthetic planner to predict
282 a synthetic route. Starting from the initial materials of this route, we then employ a reaction model to
283 simulate wet lab experiments and reproduce the synthetic route until we reach the final molecule m' .
284 Finally, we compute the Tanimoto similarity between m and m' , which we define as the round-trip
285 score. Figure 3 provides an illustration of the entire process. The round-trip score, which encapsulates
286 this process, can be mathematically expressed as follows:
287

$$288 S(m) = Sim(m, f_{\Phi}(g_{\Theta}(m))) = Sim(m, m'), \quad (1)$$

289 where g denotes the retrosynthetic planner parameterized by Φ and f represents the forward model
290 parameterized by Θ .

291 292 4 EXPERIMENTS

293 Our experiment consists of two parts. The first part focuses on assessing the reliability of the SA
294 score, search success rate, and round-trip score. The second part evaluates the synthesizability of
295 generated molecules using the round-trip score.

296 297 4.1 EVALUATING THE RELIABILITY OF SYNTHESIZABILITY METRICS

298 Currently, retrosynthetic planners are employed to generate synthetic routes for new molecules. When
299 the planner predicts a route, our synthesizability evaluation metrics need to differentiate between
300 feasible and infeasible routes. Therefore, we need a dataset to assess such discriminative capability
301 of these synthesizability evaluation metrics.

302 **Dataset Construction.** To prepare the dataset, we first clean and deduplicate the USPTO reactions,
303 resulting in approximately 916k reactions. These reactions are then used to construct a reaction
304 network. Molecules with an out-degree of 0 in the network are treated as target molecules, and
305 their corresponding synthetic routes are extracted. This process yields synthetic routes for 107,354
306 molecules, where the leaf nodes in the routes are starting materials. Note that some molecules can be
307 synthesized through multiple synthetic routes in the dataset.

308 The dataset is then divided into training, validation, and test sets, based on molecules. These splits
309 consist of 107,154, 100, and 100 data points, respectively. Each data point includes the target
310 molecule and all its associated synthetic routes.

311 **Settings.** We employ the template-based model Neuralsym as our retrosynthesis model, training it
312 on reactions derived from the 107,154 data points. For predicting synthetic routes for new molecules,
313 we leverage Neuralsym integrated with beam search as our retrosynthetic planner. We use the
314 Transformer Decoder as our forward reaction prediction model, training it on 916,000 reactions. All
315 experiments in this paper are conducted using an Nvidia H100 80G GPU. We find that the primary
316 bottleneck in time complexity during the search is Neuralsym’s retrosynthesis prediction, which
317 requires 0.157s per prediction. In contrast, our forward model, which utilizes KV cache and batch
318 decoding, achieves a rapid prediction time of only 0.0055s per reaction.

Table 1: Performance of synthesizability evaluation metrics.

Metric	Accuracy	Precision	Recall	F1 Score
Search Success Rate	-	71.6%	-	-
Round-trip Score	66.0%	81.5%	64.7%	72.0%

Evaluation Protocol. We use 100 data points from the test set to evaluate the ability of the synthesizability evaluation metric to distinguish between feasible and infeasible routes. For these 100 target molecules, we first employ the retrosynthetic planner to predict synthetic routes with a beam size of 5. During the search process, the depth of each route is restricted to not exceed the maximum depth of the reference route for the target molecule in the test set. While the planner can generate up to five different routes for each molecule, we only consider the route with the highest confidence score. Additionally, our retrosynthetic planner can’t generate routes for 5 of the molecules.

To determine the feasibility of a predicted route, we compare it against the reference routes in the test set. If the starting materials of the predicted route match the starting materials of any reference route, the route is deemed feasible. However, it is important to note that the reference routes in the test set do not cover all possible feasible routes. For predicted routes that do not match any reference route, we manually assess their feasibility using the CAS SciFinder (Gabrielson, 2018) tool² combined with our domain knowledge.

Through this process, we find that for 56 molecules, the predicted routes are identified as feasible based on the reference routes in the test set. For an additional 12 molecules, feasibility is confirmed through manual evaluation and the use of CAS tools. However, the predicted routes for the remaining 32 molecules are determined to be infeasible. We evaluate the ability of synthesizability evaluation metrics to identify two types of routes: feasible and infeasible.

For **feasible** routes, if the round-trip score is 1, it indicates that our forward reaction model successfully simulates the route to synthesize the target molecule, which is considered a successful identification. For **infeasible** routes, if the round-trip score is not 1, it indicates that the forward reaction model fails to synthesize the target molecule by simulating the route, which is also counted as a successful identification. Based on this, we define the following terms:

- **True Positive (TP):** Correctly identified feasible routes (round-trip score = 1 for actual feasible routes): 44.
- **True Negative (TN):** Correctly identified infeasible routes (round-trip score \neq 1 for actual infeasible routes): 22.
- **False Positive (FP):** Incorrectly identified feasible routes (round-trip score = 1 for actual infeasible routes): 10.
- **False Negative (FN):** Incorrectly identified infeasible routes (round-trip score \neq 1 for actual feasible routes): 24.

Since the search success rate does not evaluate the feasibility of predicted routes, we define these terms as follows:

- **True Positive (TP):** Feasible routes correctly identified as successful search: 68.
- **False Positive (FP):** Infeasible routes incorrectly identified as successful search (routes generated but are infeasible): 27.

As the SA scores of these molecules are similar, we conclude that the SA score lacks the ability to differentiate between feasible and infeasible routes. Therefore, we do not include it as a baseline. Additionally, for the search success rate, meaningful TN and FN are absent. Therefore, we use $\text{Precision} = \frac{TP}{TP+FP}$ to compare these synthesizability evaluation metrics. Besides, we provide $\text{Accuracy} = \frac{TP+TN}{TP+TN+FP+FN}$, $\text{Recall} = \frac{TP}{TP+FN}$, and $\text{F1 Score} = 2 \times \frac{\text{Precision} \times \text{Recall}}{\text{Precision} + \text{Recall}}$ for round-trip score.

²<https://scifinder-n.cas.org/>

Table 2: Performance Comparison of Various Models Using Top-k (Max > 0.9) Route Quality.

Model	Average Number of Atoms	Ratio of Starting Materials	Top-1	Top-2	Top-3	Top-4	Top-5
LiGAN	21.17	1.66%	1.95%	2.06%	2.16%	2.26%	2.29%
DecompDiff	28.34	0.53%	1.88%	2.20%	2.43%	2.47%	2.50%
TargetDiff	24.46	2.05%	2.83%	3.05%	3.18%	3.22%	3.25%
DrugGPS	23.36	5.54%	6.80%	7.19%	7.38%	7.48%	7.57%
AR	17.98	4.67%	6.75%	7.32%	7.58%	7.83%	7.96%
FLAG	22.42	10.35%	12.44%	12.96%	13.34%	13.57%	13.69%
Pocket2Mol	18.53	14.75%	18.08%	19.03%	19.44%	19.56%	19.78%

Results. Table 1 compares the precision of the search success rate and the round-trip score. The results clearly demonstrate that the round-trip score outperforms the search success rate, emphasizing the strength of the forward reaction model in assessing route feasibility. This is particularly important when minimizing false positives, as inaccurately identifying infeasible routes as feasible can compromise the reliability of the synthesizability evaluation metrics. Moreover, as more reaction data becomes available, the forward reaction model is expected to improve in accuracy, resulting in increasingly reliable round-trip score evaluations.

4.2 BENCHMARKING GENERATED MOLECULES WITH ROUND-TRIP SCORE

In this section, we utilize the round-trip score to assess the synthesizability of molecules generated by SBDD models.

Settings. We employ the same forward reaction prediction model and retrosynthesis described in Section 4.1. During the search process, we set the beam size to 5 and limit the depth of each route to a maximum of 15. Due to computational constraints, we are unable to use a beam size of 50 as employed in retrosynthesis evaluation (Dai et al., 2019). Besides, our approach generates about 5 synthetic routes per molecule, in contrast to previous methods in retrosynthetic planning that typically produce only one route. This offers a more comprehensive evaluation compared to the search success rate metric used in earlier studies (Chen et al., 2020) for evaluating search algorithms.

Baselines. For our evaluation, we employ a diverse set of state-of-the-art SBDD models, including LiGAN (Ragoza et al., 2022), AR (Luo et al., 2021), Pocket2Mol (Peng et al., 2022), FLAG (Zhang et al., 2022), TargetDiff (Guan et al., 2023a), DrugGPS (Zhang & Liu, 2023), and DecompDiff (Guan et al., 2023b). These models are trained and tested using the CrossDocked dataset (Francoeur et al., 2020), which comprises an extensive collection of 22.5 million protein-molecule structures. Our experimental setup involves randomly selecting 100,000 protein-ligand pairs from this dataset for training purposes. For testing, we draw 100 proteins from the remaining data points. To ensure a comprehensive evaluation, we randomly sample 100 molecules for each protein pocket in the test dataset, resulting in a total of 10,000 molecules. Additionally, we also verify the validity and plausibility of these molecules. After that, we employ our retrosynthetic planner to generate synthetic routes for them.

Metrics. We calculate the average number of atoms in the generated molecules and the proportion that are starting materials. Besides, we calculate the percentage of molecules for which at least one of the top-k predicted synthetic routes achieves a round-trip score exceeding 0.9.

Results. Based on the results presented in Table 2, we can draw several conclusions. There is a significant variation in performance across different SBDD models. As the average number of atoms in the generated molecules increases, the ratio of starting materials and the top-k performance. The Top-5 Max > 0.9 ranges from 2.29% for LiGAN to 19.78% for Pocket2Mol, indicating a substantial difference in the models’ abilities to generate synthetically accessible molecules. Pocket2Mol consistently outperforms other models across all metrics, with 19.78% of its generated molecules having at least one high-quality synthetic route (round-trip score > 0.9) among the top 5 predictions. The improvement in performance from Top-1 to Top-5 suggests that considering multiple top predictions can significantly increase the likelihood of finding feasible synthetic routes.

432 Notably, the performance ranking of models remains consistent across all top-k evaluations except
433 top-1. The performance increase from Top-4 to Top-5 is less than 1%, indicating that the performance
434 is approaching saturation. Additionally, as shown in Table 4 in Appendix B, the performance gap
435 between models generally widens as k increases, with most gaps showing an upward trend. These
436 observations suggest that our chosen beam size of 5 is sufficient to provide an accurate ranking of
437 each model’s performance. This consistency in ranking and the approaching saturation point lend
438 credibility to our evaluation methodology and the reliability of our comparative analysis. More
439 experiment results can be found in Appendix B. The analysis of molecular properties from various
440 generative models, as presented in Table 7, reveals that superior molecular properties do not always
441 correlate with better synthesizability. Even for the best-performing model, a considerable portion
442 of generated molecules still lack high-quality synthetic routes, indicating room for improvement
443 in generating synthetically accessible molecules in SBDD tasks. These findings underscore the
444 importance of evaluating synthetic accessibility in SBDD models and highlight the potential of using
445 top-k predictions to identify feasible synthetic routes for generated molecules.

446 5 RELATED WORK

448 **Structured-Based Drug Design.** Generative models for Structure-Based Drug Design (SBDD) can
449 be broadly categorized into two main types: non-diffusion and diffusion-based models. Non-diffusion
450 models encompass a range of approaches, including LiGAN (Ragoza et al., 2022), AR (Luo et al.,
451 2021), Pocket2Mol (Peng et al., 2022), GraphBP (Liu et al., 2022b), FLAG (Zhang et al., 2022),
452 and DrugGPS (Zhang & Liu, 2023). On the other hand, diffusion-based models can be considered
453 as an alternative, such as TargetDiff (Guan et al., 2023a), DiffSBDD (Schneuing et al., 2022), and
454 DecompDiff (Guan et al., 2023b).

456 **Reaction Prediction Model.** Reaction prediction models can be broadly categorized into two
457 approaches: template-based and template-free. Template-based methods (Wei et al., 2016; Segler
458 & Waller, 2017; Qian et al., 2020; Chen & Jung, 2022) begin by extracting reaction templates
459 $T = \{T_1, \dots, T_{N(T)}\}$ from a reaction database. These methods then predict the most suitable
460 template class based on the given reactants and apply the predefined, encoded template to generate the
461 product. Template-free approaches, on the other hand, are more diverse. Some, inspired by chemical
462 reaction mechanisms, adopt a two-stage learning process (Jin et al., 2017). They first identify the
463 chemical reaction centers of the reactants using atom mapping numbers, and then form new bonds or
464 break existing ones between atoms at these centers. However, most contemporary strategies employ
465 an end-to-end, template-free learning paradigm for reaction prediction. Several methods (Yang et al.,
466 2019; Schwaller et al., 2019a; Tetko et al., 2020; Irwin et al., 2022; Lu & Zhang, 2022; Zhao et al.,
467 2022; Tu & Coley, 2022) frame reaction prediction as a sequence-to-sequence or graph-to-sequence
468 problem. Other approaches (Bradshaw et al., 2019; Do et al., 2019; Sacha et al., 2021; Bi et al., 2021;
469 Meng et al., 2023) predict the product by directly performing graph transformations on the reactants’
470 graph representations.

471 **Retrosynthesis Model.** Existing retrosynthesis models (Segler & Waller, 2017; Coley et al., 2017;
472 Liu et al., 2017; Zheng et al., 2019; Chen et al., 2019; Dai et al., 2019; Karpov et al., 2019; Chen
473 et al., 2020; Ishiguro et al., 2020; Guo et al., 2020; Tetko et al., 2020; Shi et al., 2020; Yan et al.,
474 2020; Seo et al., 2021; Chen & Jung, 2021; Lee et al., 2021; Seidl et al., 2021; Somnath et al., 2021;
475 Sun et al., 2021; Yan et al., 2022; Fang et al., 2022; Gao et al., 2022b; Wan et al., 2022; He et al.,
476 2022; Liu et al., 2022a; Tu & Coley, 2022; Lin et al., 2022; Zhong et al., 2022; Baker et al., 2023;
477 Zhong et al., 2023; Yu et al., 2023; Li et al., 2023b; Xie et al., 2023; Sacha et al., 2023; Zhu et al.,
478 2023b; Jiang et al., 2023; Qian et al., 2023; Xiong et al., 2023; Wang et al., 2023; Gao et al., 2023;
479 Zhu et al., 2023a; Lan et al., 2023; Chen et al., 2023; Yao et al., 2023; Lin et al., 2023; Liu et al.,
480 2024b; Zhang et al., 2024b;a; Lan et al., 2024) can be broadly categorized into three main types:
481 template-free, semi-template-based, and template-based methods. These categories can be further
482 refined based on their utilization of atom mapping information. Template-free methods typically
483 approach retrosynthesis as either a translation problem (Karpov et al., 2019) or a graph edit problem
484 (Sacha et al., 2021). Some of these methods optionally use atom mapping to align input and output
485 molecules (Seo et al., 2021; Zhong et al., 2022; Yao et al., 2023). Template-based methods (Segler
& Waller, 2017; Dai et al., 2019) leverage atom mapping information to create a pool of reaction
templates. They generally frame retrosynthesis as a template classification or retrieval problem.

486 Semi-template-based methods (Shi et al., 2020; Somnath et al., 2021) also utilize atom mapping
487 information, but they employ it to obtain other prior information, such as identifying reaction centers.
488 Many of these methods adopt a two-stage learning paradigm for retrosynthesis: First, they identify
489 the reaction center in the product molecule and break it into synthons. Then, they transform these
490 synthons into reactants.

491
492 **Search Algorithm.** A variety of search algorithms have been developed to navigate the synthetic
493 planning. These include beam search, neural A* search (Chen et al., 2020; Han et al., 2022; Xie et al.,
494 2022), Monte Carlo Tree Search (MCTS) (Segler et al., 2018; Hong et al., 2021), and reinforcement
495 learning-based (RL-based) search (Yu et al., 2022). Some other works to this field include (Kishimoto
496 et al., 2019; Heifets & Jurisica, 2012; Kim et al., 2021; Hassen et al., 2022; Li et al., 2023a; Zhang
497 et al., 2023; Liu et al., 2023a; Lee et al., 2023; Yuan et al., 2024; Tripp et al., 2024). These algorithms
498 are designed to explore the vast reaction space, prioritizing the most promising synthetic routes.

500 6 CONCLUSION

501
502 In this work, we propose a novel round-trip score to assess the synthesizability of molecules generated
503 by existing SBDD models. This score evaluates the likelihood that a retrosynthetic planner, trained
504 on current reaction data, can predict feasible synthetic routes for these molecules. To enhance the
505 robustness of our evaluation method, we advocate for the release of additional reaction data. This
506 expanded dataset would significantly improve the accuracy and reliability of our assessments.

508 REFERENCES

- 509
510 Frazier N Baker, Ziqi Chen, and Xia Ning. Rlsync: Offline-online reinforcement learning for synthon
511 completion. *arXiv preprint arXiv:2309.02671*, 2023.
- 512 Hangrui Bi, Hengyi Wang, Chence Shi, Connor Coley, Jian Tang, and Hongyu Guo. Non-
513 autoregressive electron redistribution modeling for reaction prediction. In *International Conference*
514 *on Machine Learning*, 2021.
- 515
516 John Bradshaw, Matt J. Kusner, Brooks Paige, Marwin H. S. Segler, and José Miguel Hernández-
517 Lobato. A generative model for electron paths. In *International Conference on Learning Representations*,
518 2019.
- 519
520 Benson Chen, Tianxiao Shen, Tommi S Jaakkola, and Regina Barzilay. Learning to make generaliz-
521 able and diverse predictions for retrosynthesis. *arXiv preprint arXiv:1910.09688*, 2019.
- 522
523 Binghong Chen, Chengtao Li, Hanjun Dai, and Le Song. Retro*: learning retrosynthetic planning
524 with neural guided a* search. In *International Conference on Machine Learning*, 2020.
- 525
526 Shuan Chen and Yousung Jung. Deep retrosynthetic reaction prediction using local reactivity and
527 global attention. *JACS Au*, 1(10):1612–1620, 2021.
- 528
529 Shuan Chen and Yousung Jung. A generalized-template-based graph neural network for accurate
530 organic reactivity prediction. *Nature Machine Intelligence*, 4(9):772–780, 2022.
- 531
532 Ziqi Chen, Oluwatosin R Ayinde, James R Fuchs, Huan Sun, and Xia Ning. G2retro as a two-step
533 graph generative models for retrosynthesis prediction. *Communications Chemistry*, 6(1):102, 2023.
- 534
535 Connor W Coley, Luke Rogers, William H Green, and Klavs F Jensen. Computer-assisted retrosyn-
536 thesis based on molecular similarity. *ACS Central Science*, 3(12):1237–1245, 2017.
- 537
538 Miruna Cretu, Charles Harris, Julien Roy, Emmanuel Bengio, and Pietro Liò. Synflownet: Towards
539 molecule design with guaranteed synthesis pathways. In *ICLR 2024 Workshop on Generative and*
Experimental Perspectives for Biomolecular Design, 2024.
- 540
541 Hanjun Dai, Chengtao Li, Connor Coley, Bo Dai, and Le Song. Retrosynthesis prediction with
542 conditional graph logic network. In *Advances in Neural Information Processing Systems*, 2019.

- 540 Kien Do, Truyen Tran, and Svetha Venkatesh. Graph transformation policy network for chemical
541 reaction prediction. In *Proceedings of the 25th ACM SIGKDD International Conference on*
542 *Knowledge Discovery & Data Mining*, 2019.
- 543
- 544 Peter Ertl and Ansgar Schuffenhauer. Estimation of synthetic accessibility score of drug-like
545 molecules based on molecular complexity and fragment contributions. *Journal of Cheminformatics*,
546 1(1):1–11, 2009.
- 547 Lei Fang, Junren Li, Ming Zhao, Li Tan, and Jian-Guang Lou. Leveraging reaction-aware substructures
548 for retrosynthesis analysis. *arXiv preprint arXiv:2204.05919*, 2022.
- 549
- 550 Paul G Francoeur, Tomohide Masuda, Jocelyn Sunseri, Andrew Jia, Richard B Iovanisci, Ian Snyder,
551 and David R Koes. Three-dimensional convolutional neural networks and a cross-docked data set
552 for structure-based drug design. *Journal of Chemical Information and Modeling*, 60(9):4200–4215,
553 2020.
- 554 Stephen Walter Gabrielson. Scifinder. *Journal of the Medical Library Association: JMLA*, 106(4):
555 588, 2018.
- 556
- 557 Wenhao Gao and Connor W Coley. The synthesizability of molecules proposed by generative models.
558 *Journal of Chemical Information and Modeling*, 60(12):5714–5723, 2020.
- 559
- 560 Wenhao Gao, Rocío Mercado, and Connor W. Coley. Amortized tree generation for bottom-up
561 synthesis planning and synthesizable molecular design. In *International Conference on Learning*
562 *Representations*, 2022a.
- 563 Zhangyang Gao, Cheng Tan, Lirong Wu, and Stan Z Li. Semiretro: Semi-template framework boosts
564 deep retrosynthesis prediction. *arXiv preprint arXiv:2202.08205*, 2022b.
- 565
- 566 Zhangyang Gao, Xingran Chen, Cheng Tan, and Stan Z Li. Motifretro: Exploring the
567 combinability-consistency trade-offs in retrosynthesis via dynamic motif editing. *arXiv preprint*
568 *arXiv:2305.15153*, 2023.
- 569 Samuel Genheden, Amol Thakkar, Veronika Chadimová, Jean-Louis Reymond, Ola Engkvist, and
570 Esben Bjerrum. Aizynthfinder: a fast, robust and flexible open-source software for retrosynthetic
571 planning. *Journal of Cheminformatics*, 12(1):1–9, 2020.
- 572
- 573 Jiaqi Guan, Wesley Wei Qian, Xingang Peng, Yufeng Su, Jian Peng, and Jianzhu Ma. 3d equivariant
574 diffusion for target-aware molecule generation and affinity prediction. In *International Conference*
575 *on Learning Representations*, 2023a.
- 576 Jiaqi Guan, Xiangxin Zhou, Yuwei Yang, Yu Bao, Jian Peng, Jianzhu Ma, Qiang Liu, Liang Wang,
577 and Quanquan Gu. DecompDiff: Diffusion models with decomposed priors for structure-based
578 drug design. In *International Conference on Machine Learning*, 2023b.
- 579
- 580 Zhongliang Guo, Stephen Wu, Mitsuru Ohno, and Ryo Yoshida. Bayesian algorithm for retrosynthesis.
581 *Journal of Chemical Information and Modeling*, 60(10):4474–4486, 2020.
- 582
- 583 Peng Han, Peilin Zhao, Chan Lu, Junzhou Huang, Jiayang Wu, Shuo Shang, Bin Yao, and Xiangliang
584 Zhang. Gnn-retro: Retrosynthetic planning with graph neural networks. In *Proceedings of the*
585 *AAAI Conference on Artificial Intelligence*, 2022.
- 586
- 587 Alan Kai Hassen, Paula Torren-Peraire, Samuel Genheden, Jonas Verhoeven, Mike Preuss, and
588 Igor Tetko. Mind the retrosynthesis gap: Bridging the divide between single-step and multi-step
retrosynthesis prediction. *arXiv preprint arXiv:2212.11809*, 2022.
- 589
- 590 Hua-Rui He, Jie Wang, Yunfei Liu, and Feng Wu. Modeling diverse chemical reactions for single-
591 step retrosynthesis via discrete latent variables. In *Proceedings of the 31st ACM International*
592 *Conference on Information & Knowledge Management*, 2022.
- 593
- Abraham Heifets and Igor Jurisica. Construction of new medicines via game proof search. In
Proceedings of the AAAI Conference on Artificial Intelligence, 2012.

- 594 Jack Hessel, Ari Holtzman, Maxwell Forbes, Ronan Le Bras, and Yejin Choi. Clipscore: A reference-
595 free evaluation metric for image captioning. *arXiv preprint arXiv:2104.08718*, 2021.
- 596
- 597 Siqi Hong, Hankz Hankui Zhuo, Kebin Jin, and Zhanwen Zhou. Retrosynthetic planning with
598 experience-guided monte carlo tree search. *arXiv preprint arXiv:2112.06028*, 2021.
- 599
- 600 Ross Irwin, Spyridon Dimitriadis, Jiazhen He, and Esben Jannik Bjerrum. Chemformer: a pre-trained
601 transformer for computational chemistry. *Machine Learning: Science and Technology*, 3(1):
602 015022, 2022.
- 603
- 604 Katsuhiko Ishiguro, Kazuya Ujihara, Ryohto Sawada, Hirotaka Akita, and Masaaki Kotera. Data
605 transfer approaches to improve seq-to-seq retrosynthesis. *arXiv preprint arXiv:2010.00792*, 2020.
- 606
- 607 Yinjie Jiang, WEI Ying, Fei Wu, Zhengxing Huang, Kun Kuang, and Zhihua Wang. Learning
608 chemical rules of retrosynthesis with pre-training. In *Proceedings of the AAAI Conference on
609 Artificial Intelligence*, 2023.
- 610
- 611 Wengong Jin, Connor Coley, Regina Barzilay, and Tommi Jaakkola. Predicting organic reaction
612 outcomes with weisfeiler-lehman network. In *Advances in Neural Information Processing Systems*,
613 2017.
- 614
- 615 Pavel Karpov, Guillaume Godin, and Igor V Tetko. A transformer model for retrosynthesis. In
616 *International Conference on Artificial Neural Networks*, 2019.
- 617
- 618 Junsu Kim, Sungsoo Ahn, Hankook Lee, and Jinwoo Shin. Self-improved retrosynthetic planning. In
619 *International Conference on Machine Learning*, 2021.
- 620
- 621 Akihiro Kishimoto, Beat Buesser, Bei Chen, and Adi Botea. Depth-first proof-number search
622 with heuristic edge cost and application to chemical synthesis planning. In *Advances in Neural
623 Information Processing Systems*, 2019.
- 624
- 625 Zixun Lan, Zuo Zeng, Binjie Hong, Zhenfu Liu, and Fei Ma. Rresearcher: Reaction center identifica-
626 tion in retrosynthesis via deep q-learning. *arXiv preprint arXiv:2301.12071*, 2023.
- 627
- 628 Zixun Lan, Binjie Hong, Jiajun Zhu, Zuo Zeng, Zhenfu Liu, Limin Yu, and Fei Ma. Retrosynthesis
629 prediction via search in (hyper) graph. *arXiv preprint arXiv:2402.06772*, 2024.
- 630
- 631 Hankook Lee, Sungsoo Ahn, Seung-Woo Seo, You Young Song, Eunho Yang, Sung-Ju Hwang, and
632 Jinwoo Shin. Retcl: A selection-based approach for retrosynthesis via contrastive learning. *arXiv
633 preprint arXiv:2105.00795*, 2021.
- 634
- 635 Seul Lee, Taein Kim, Min-Soo Choi, Yejin Kwak, Jeongbin Park, Sung Ju Hwang, and Sang-Gyu
636 Kim. Readretro: Natural product biosynthesis planning with retrieval-augmented dual-view
637 retrosynthesis. *bioRxiv*, pp. 2023–03, 2023.
- 638
- 639 Junren Li, Lei Fang, and Jian-Guang Lou. Retro-bleu: Quantifying chemical plausibility of ret-
640 rosynthesis routes through reaction template sequence analysis. *arXiv preprint arXiv:2311.06304*,
641 2023a.
- 642
- 643 Junren Li, Lei Fang, and Jian-Guang Lou. Retroranker: leveraging reaction changes to improve
644 retrosynthesis prediction through re-ranking. *Journal of Cheminformatics*, 15(1):58, 2023b.
- 645
- 646 Min Htoo Lin, Zhengkai Tu, and Connor W Coley. Improving the performance of models for one-step
647 retrosynthesis through re-ranking. *Journal of Cheminformatics*, 14(1):1–13, 2022.
- 648
- 649 Zaiyun Lin, Shiqiu Yin, Lei Shi, Wenbiao Zhou, and Yingsheng John Zhang. G2gt: Retrosynthesis
650 prediction with graph-to-graph attention neural network and self-training. *Journal of Chemical
651 Information and Modeling*, 63(7):1894–1905, 2023.
- 652
- 653 Christopher A Lipinski. Lead-and drug-like compounds: the rule-of-five revolution. *Drug Discovery
654 Today: Technologies*, 1(4):337–341, 2004.
- 655
- 656 Bowen Liu, Bharath Ramsundar, Prasad Kawthekar, Jade Shi, Joseph Gomes, Quang Luu Nguyen,
657 Stephen Ho, Jack Sloane, Paul Wender, and Vijay Pande. Retrosynthetic reaction prediction using
658 neural sequence-to-sequence models. *ACS Central Science*, 3(10):1103–1113, 2017.

- 648 Guoqing Liu, Di Xue, Shufang Xie, Yingce Xia, Austin Tripp, Krzysztof Maziarz, Marwin Segler,
649 Tao Qin, Zongzhang Zhang, and Tie-Yan Liu. Retrosynthetic planning with dual value networks.
650 In *International Conference on Machine Learning*, 2023a.
- 651
- 652 Jiahao Liu, Chaochao Yan, Yang Yu, Chan Lu, Junzhou Huang, Le Ou-Yang, and Peilin Zhao. Mars:
653 A motif-based autoregressive model for retrosynthesis prediction. *arXiv preprint arXiv:2209.13178*,
654 2022a.
- 655 Meng Liu, Youzhi Luo, Kanji Uchino, Koji Maruhashi, and Shuiwang Ji. Generating 3d molecules
656 for target protein binding. In *International Conference on Machine Learning*, 2022b.
- 657
- 658 Songtao Liu, Zhengkai Tu, Minkai Xu, Zuobai Zhang, Lu Lin, Rex Ying, Jian Tang, Peilin Zhao, and
659 Dinghao Wu. Fusionretro: Molecule representation fusion via in-context learning for retrosynthetic
660 planning. In *International Conference on Machine Learning*, 2023b.
- 661 Songtao Liu, Hanjun Dai, Yue Zhao, and Peng Liu. Preference optimization for molecule synthesis
662 with conditional residual energy-based models. In *International Conference on Machine Learning*,
663 2024a.
- 664
- 665 Yifeng Liu, Hanwen Xu, Tangqi Fang, Haocheng Xi, Zixuan Liu, Sheng Zhang, Hoifung Poon, and
666 Sheng Wang. T-rex: Text-assisted retrosynthesis prediction. *arXiv preprint arXiv:2401.14637*,
667 2024b.
- 668
- 669 DM Lowe. Patent reaction extraction: downloads, 2014.
- 670 Jieyu Lu and Yingkai Zhang. Unified deep learning model for multitask reaction predictions with
671 explanation. *Journal of Chemical Information and Modeling*, 62(6):1376–1387, 2022.
- 672
- 673 Shitong Luo, Jiaqi Guan, Jianzhu Ma, and Jian Peng. A 3d generative model for structure-based drug
674 design. In *Advances in Neural Information Processing Systems*, 2021.
- 675 Ziqiao Meng, Peilin Zhao, Yang Yu, and Irwin King. Doubly stochastic graph-based non-
676 autoregressive reaction prediction. In *International Joint Conference on Artificial Intelligence*,
677 2023.
- 678
- 679 Maud Parrot, Hamza Tajmouati, Vinicius Barros Ribeiro da Silva, Brian Ross Atwood, Robin
680 Fourcade, Yann Gaston-Mathé, Nicolas Do Huu, and Quentin Perron. Integrating synthetic
681 accessibility with ai-based generative drug design. *Journal of Cheminformatics*, 15(1):83, 2023.
- 682 Adam Paszke, Sam Gross, Francisco Massa, Adam Lerer, James Bradbury, Gregory Chanan, Trevor
683 Killeen, Zeming Lin, Natalia Gimelshein, Luca Antiga, et al. Pytorch: An imperative style,
684 high-performance deep learning library. In *Advances in Neural Information Processing Systems*,
685 2019.
- 686
- 687 Ian Paterson and Edward A Anderson. The renaissance of natural products as drug candidates.
688 *Science*, 310(5747):451–453, 2005.
- 689 Xingang Peng, Shitong Luo, Jiaqi Guan, Qi Xie, Jian Peng, and Jianzhu Ma. Pocket2mol: Efficient
690 molecular sampling based on 3d protein pockets. In *International Conference on Machine Learning*,
691 2022.
- 692
- 693 Wesley Wei Qian, Nathan T Russell, Claire LW Simons, Yunan Luo, Martin D Burke, and Jian
694 Peng. Integrating deep neural networks and symbolic inference for organic reactivity prediction.
695 *ChemRxiv*, 2020.
- 696
- 697 Yujie Qian, Zhening Li, Zhengkai Tu, Connor W Coley, and Regina Barzilay. Predictive chemistry
698 augmented with text retrieval. *arXiv preprint arXiv:2312.04881*, 2023.
- 699
- 700 Alec Radford, Jong Wook Kim, Chris Hallacy, Aditya Ramesh, Gabriel Goh, Sandhini Agarwal,
701 Girish Sastry, Amanda Askell, Pamela Mishkin, Jack Clark, et al. Learning transferable visual
models from natural language supervision. In *International Conference on Machine Learning*,
2021.

- 702 Matthew Ragoza, Tomohide Masuda, and David Ryan Koes. Generating 3d molecules conditional on
703 receptor binding sites with deep generative models. *Chemical Science*, 13(9):2701–2713, 2022.
704
- 705 Mikołaj Sacha, Mikołaj Błaz, Piotr Byrski, Paweł Dabrowski-Tumanski, Mikołaj Chrominski, Rafał
706 Loska, Paweł Włodarczyk-Pruszynski, and Stanisław Jastrzebski. Molecule edit graph atten-
707 tion network: modeling chemical reactions as sequences of graph edits. *Journal of Chemical*
708 *Information and Modeling*, 61(7):3273–3284, 2021.
- 709 Mikołaj Sacha, Michał Sadowski, Piotr Kozakowski, Ruard van Workum, and Stanisław Jastrzeb-
710 ski. Molecule-edit templates for efficient and accurate retrosynthesis prediction. *arXiv preprint*
711 *arXiv:2310.07313*, 2023.
712
- 713 Arne Schneuing, Yuanqi Du, Charles Harris, Arian Jamasb, Ilia Igashov, Weitao Du, Tom Blundell,
714 Pietro Lió, Carla Gomes, Max Welling, et al. Structure-based drug design with equivariant diffusion
715 models. *arXiv preprint arXiv:2210.13695*, 2022.
- 716 Philippe Schwaller, Teodoro Laino, Théophile Gaudin, Peter Bolgar, Christopher A Hunter, Costas
717 Bekas, and Alpha A Lee. Molecular transformer: a model for uncertainty-calibrated chemical
718 reaction prediction. *ACS Central Science*, 5(9):1572–1583, 2019a.
719
- 720 Philippe Schwaller, R Petraglia, VH Nair, and Teodoro Laino. Evaluation metrics for single-step
721 retrosynthetic models. In *Second Workshop on Machine Learning and the Physical Sciences*
722 *(NeurIPS 2019)*, 2019b.
- 723 Marwin HS Segler and Mark P Waller. Neural-symbolic machine learning for retrosynthesis and
724 reaction prediction. *Chemistry—A European Journal*, 23(25):5966–5971, 2017.
725
- 726 Marwin HS Segler, Mike Preuss, and Mark P Waller. Planning chemical syntheses with deep neural
727 networks and symbolic ai. *Nature*, 555(7698):604, 2018.
728
- 729 Philipp Seidl, Philipp Renz, Natalia Dyubankova, Paulo Neves, Jonas Verhoeven, Jörg K Wegner,
730 Sepp Hochreiter, and Günter Klambauer. Modern hopfield networks for few-and zero-shot reaction
731 prediction. *arXiv preprint arXiv:2104.03279*, 2021.
- 732 Seung-Woo Seo, You Young Song, June Yong Yang, Seohui Bae, Hankook Lee, Jinwoo Shin, Sung Ju
733 Hwang, and Eunho Yang. Gta: Graph truncated attention for retrosynthesis. In *Proceedings of the*
734 *AAAI Conference on Artificial Intelligence*, 2021.
735
- 736 Chence Shi, Minkai Xu, Hongyu Guo, Ming Zhang, and Jian Tang. A graph to graphs framework for
737 retrosynthesis prediction. In *International Conference on Machine Learning*, 2020.
- 738 Vignesh Ram Somnath, Charlotte Bunne, Connor Coley, Andreas Krause, and Regina Barzilay.
739 Learning graph models for retrosynthesis prediction. In *Advances in Neural Information Processing*
740 *Systems*, 2021.
741
- 742 Teague Sterling and John J Irwin. Zinc 15–ligand discovery for everyone. *Journal of Chemical*
743 *Information and Modeling*, 55(11):2324–2337, 2015.
- 744 Ruoxi Sun, Hanjun Dai, Li Li, Steven Kearnes, and Bo Dai. Towards understanding retrosynthesis by
745 energy-based models. In *Advances in Neural Information Processing Systems*, 2021.
746
- 747 Igor V Tetko, Pavel Karpov, Ruud Van Deursen, and Guillaume Godin. State-of-the-art augmented
748 nlp transformer models for direct and single-step retrosynthesis. *Nature Communications*, 11(1):
749 1–11, 2020.
- 750 Austin Tripp, Krzysztof Maziarz, Sarah Lewis, Guoqing Liu, and Marwin Segler. Re-evaluating
751 chemical synthesis planning algorithms. In *NeurIPS 2022 AI for Science: Progress and Promises*,
752 2022.
753
- 754 Austin Tripp, Krzysztof Maziarz, Sarah Lewis, Marwin Segler, and José Miguel Hernández-Lobato.
755 Retro-fallback: retrosynthetic planning in an uncertain world. In *International Conference on*
Learning Representations, 2024.

- 756 Zhengkai Tu and Connor W Coley. Permutation invariant graph-to-sequence model for template-free
757 retrosynthesis and reaction prediction. *Journal of Chemical Information and Modeling*, 62(15):
758 3503–3513, 2022.
- 759 Yue Wan, Chang-Yu Hsieh, Ben Liao, and Shengyu Zhang. Retroformer: Pushing the limits of
760 end-to-end retrosynthesis transformer. In *International Conference on Machine Learning*, 2022.
- 761
- 762 Yiming Wang, Yuxuan Song, Minkai Xu, Rui Wang, Hao Zhou, and Weiyang Ma. RetroDiff:
763 Retrosynthesis as multi-stage distribution interpolation. *arXiv preprint arXiv:2311.14077*, 2023.
- 764
- 765 Jennifer N Wei, David Duvenaud, and Alán Aspuru-Guzik. Neural networks for the prediction of
766 organic chemistry reactions. *ACS Central Science*, 2(10):725–732, 2016.
- 767 Shufang Xie, Rui Yan, Peng Han, Yingce Xia, Lijun Wu, Chenjuan Guo, Bin Yang, and Tao Qin.
768 Retrograph: Retrosynthetic planning with graph search. In *Proceedings of the 28th ACM SIGKDD*
769 *Conference on Knowledge Discovery and Data Mining*, 2022.
- 770
- 771 Shufang Xie, Rui Yan, Junliang Guo, Yingce Xia, Lijun Wu, and Tao Qin. Retrosynthesis prediction
772 with local template retrieval. *arXiv preprint arXiv:2306.04123*, 2023.
- 773 Jiacheng Xiong, Wei Zhang, Zunyun Fu, Jiatao Huang, Xiangtai Kong, Yitian Wang, Zhaoping
774 Xiong, and Mingyue Zheng. Improve retrosynthesis planning with a molecular editing language.
775 *ChemRxiv*, 2023.
- 776
- 777 Chaochao Yan, Qianggang Ding, Peilin Zhao, Shuangjia Zheng, Jinyu Yang, Yang Yu, and Junzhou
778 Huang. Retroxpert: Decompose retrosynthesis prediction like a chemist. In *Advances in Neural*
779 *Information Processing Systems*, 2020.
- 780 Chaochao Yan, Peilin Zhao, Chan Lu, Yang Yu, and Junzhou Huang. Retrocomposer: Composing
781 templates for template-based retrosynthesis prediction. *Biomolecules*, 12(9):1325, 2022.
- 782
- 783 Qingyi Yang, Vishnu Sresht, Peter Bolgar, Xinjun Hou, Jacquelyn L Klug-McLeod, Christopher R
784 Butler, et al. Molecular transformer unifies reaction prediction and retrosynthesis across pharma
785 chemical space. *Chemical Communications*, 55(81):12152–12155, 2019.
- 786 Lin Yao, Zhen Wang, Wentao Guo, Shang Xiang, Wentan Liu, and Guolin Ke. Node-aligned
787 graph-to-graph generation for retrosynthesis prediction. *arXiv preprint arXiv:2309.15798*, 2023.
- 788
- 789 Jiaxuan You, Bowen Liu, Zhitao Ying, Vijay Pande, and Jure Leskovec. Graph convolutional
790 policy network for goal-directed molecular graph generation. In *Advances in Neural Information*
791 *Processing Systems*, 2018.
- 792 Yemin Yu, Ying Wei, Kun Kuang, Zhengxing Huang, Huaxiu Yao, and Fei Wu. Grasp: Navigating
793 retrosynthetic planning with goal-driven policy. In *Advances in Neural Information Processing*
794 *Systems*, 2022.
- 795 Yemin Yu, Luotian Yuan, Ying Wei, Hanyu Gao, Xinhai Ye, Zhihua Wang, and Fei Wu. Retroood:
796 Understanding out-of-distribution generalization in retrosynthesis prediction. *arXiv preprint*
797 *arXiv:2312.10900*, 2023.
- 798
- 799 Luotian Yuan, Yemin Yu, Ying Wei, Yongwei Wang, Zhihua Wang, and Fei Wu. Active retrosynthetic
800 planning aware of route quality. In *International Conference on Learning Representations*, 2024.
- 801 Qiang Zhang, Juan Liu, Wen Zhang, Feng Yang, Zhihui Yang, and Xiaolei Zhang. A multi-stream
802 network for retrosynthesis prediction. *Frontiers of Computer Science*, 18(2):182906, 2024a.
- 803
- 804 Xu Zhang, Yiming Mo, Wenguan Wang, and Yi Yang. Retrosynthesis prediction enhanced by in-silico
805 reaction data augmentation. *arXiv preprint arXiv:2402.00086*, 2024b.
- 806 Yan Zhang, Hao Hao, Xiao He, Shuanhu Gao, and Aimin Zhou. Evolutionary retrosynthetic route
807 planning. *arXiv preprint arXiv:2310.05186*, 2023.
- 808
- 809 Zaixi Zhang and Qi Liu. Learning subpocket prototypes for generalizable structure-based drug design.
In *International Conference on Machine Learning*, 2023.

810 Zaixi Zhang, Yaosen Min, Shuxin Zheng, and Qi Liu. Molecule generation for target protein binding
811 with structural motifs. In *International Conference on Learning Representations*, 2022.
812

813 Ming Zhao, Lei Fang, Li Tan, Jian-Guang Lou, and Yves Lepage. Leveraging reaction-aware
814 substructures for retrosynthesis and reaction prediction. *arXiv preprint arXiv:2204.05919*, 2022.

815 Shuangjia Zheng, Jiahua Rao, Zhongyue Zhang, Jun Xu, and Yuedong Yang. Predicting retrosynthetic
816 reactions using self-corrected transformer neural networks. *Journal of Chemical Information and
817 Modeling*, 60(1):47–55, 2019.
818

819 Shuangjia Zheng, Tao Zeng, Chengtao Li, Binghong Chen, Connor W Coley, Yuedong Yang, and
820 Ruibo Wu. Deep learning driven biosynthetic pathways navigation for natural products with
821 bionavi-np. *Nature Communications*, 13(1):3342, 2022.

822 Weihe Zhong, Ziduo Yang, and Calvin Yu-Chian Chen. Retrosynthesis prediction using an end-to-end
823 graph generative architecture for molecular graph editing. *Nature Communications*, 14(1):3009,
824 2023.

825 Zipeng Zhong, Jie Song, Zunlei Feng, Tiantao Liu, Lingxiang Jia, Shaolun Yao, Min Wu, Tingjun
826 Hou, and Mingli Song. Root-aligned smiles: a tight representation for chemical reaction prediction.
827 *Chemical Science*, 13(31):9023–9034, 2022.
828

829 Jiajun Zhu, Binjie Hong, Zixun Lan, and Fei Ma. Single-step retrosynthesis via reaction center and
830 leaving groups prediction. In *2023 16th International Congress on Image and Signal Processing,
831 BioMedical Engineering and Informatics*, 2023a.

832 Jinhua Zhu, Yingce Xia, Lijun Wu, Shufang Xie, Wengang Zhou, Tao Qin, Houqiang Li, and Tie-Yan
833 Liu. Dual-view molecular pre-training. In *Proceedings of the 29th ACM SIGKDD Conference on
834 Knowledge Discovery and Data Mining*, 2023b.
835
836
837
838
839
840
841
842
843
844
845
846
847
848
849
850
851
852
853
854
855
856
857
858
859
860
861
862
863

864 A REPRODUCIBILITY

865
866 We use Pytorch (Paszke et al., 2019) to implement our retrosynthesis and reaction prediction models.
867 The softwares that we use for experiments are Python 3.6.8, CUDA 10.2.89, CUDNN 7.6.5, einops
868 0.4.1, pytorch 1.9.0, pytorch-scatter 2.0.9, pytorch-sparse 0.6.12, numpy 1.19.2, torchvision 0.10.0,
869 and torchdrug 0.1.3.

870
871 Table 3: The hyper-parameters for the reaction model.

873	max length	402
874	embedding size	64
875	decoder layers	6
876	attention heads	8
877	FFN hidden	2048
878	dropout	0.1
879	epochs	2000
880	batch size	128
881	warmup	16000
882	lr factor	20
883	scheduling	$lr = \frac{\text{lr factor} \times \min(1.0, \frac{0.1 \text{ num_step}}{\text{warmup}})}{\max(0.1 \text{ num_step}, \text{warmup})}$

884
885 Table 3 reports the hyper-parameter setting of our reaction model. For Neuralsym, we follow the
886 setting in <https://github.com/linminhtoo/neuralsym>.

887 B ADDITIONAL EXPERIMENTAL RESULTS

888 B.1 SYNTHESIZABILITY EVALUATION

889
890 Tables 4 and 6 present performance gaps between consecutive models for top-k metrics with thresholds
891 of 0.9 and 0.8, respectively. Table 5 compares model performance using top-k route quality with a
892 threshold of 0.8.

893
894 Table 4: Performance Gaps (%) Between Consecutive Models for Top-k (Max > 0.9) Metrics

896	Gap Between Models	Top-1	Top-2	Top-3	Top-4	Top-5
897	LiGAN to DecompDiff	-0.07	0.14	0.27	0.21	0.21
898	DecompDiff to TargetDiff	0.95	0.85	0.75	0.75	0.75
899	TargetDiff to DrugGPS	3.97	4.14	4.20	4.26	4.32
900	DrugGPS to AR	-0.05	0.13	0.20	0.35	0.39
901	AR to FLAG	5.69	5.64	5.76	5.74	5.73
902	FLAG to Pocket2Mol	5.64	6.07	6.10	5.99	6.09

903
904 Table 5: Performance (%) Comparison of Various Models Using Top-k Route Quality (Max > 0.8).

905	Model	Top-1	Top-2	Top-3	Top-4	Top-5
906	LiGAN	2.05	2.16	2.27	2.37	2.42
907	DecompDiff	2.36	2.77	3.04	3.18	3.27
908	TargetDiff	2.86	3.09	3.22	3.27	3.31
909	DrugGPS	7.03	7.46	7.68	7.81	7.92
910	AR	6.96	7.69	7.99	8.28	8.46
911	FLAG	12.74	13.40	13.85	14.13	14.33
912	Pocket2Mol	18.66	19.77	20.27	20.44	20.65

913
914 The properties of generated molecules presented in Table 7 are derived from two primary sources.
915 For LiGAN, AR, Pocket2Mol, FLAG, and DrugGPS, all reported metrics (Vina Score, High Affinity,
916 QED, SA, LogP, Lip., Sim. Train, and Div.) are extracted from the DrugGPS paper. For TargetDiff
917 and DecompDiff, the Vina Score, High Affinity, QED, SA, and Div. metrics are sourced from the
DecompDiff paper.

Table 6: Performance Gaps (%) Between Consecutive Models for Top-k (Max > 0.8) Metrics

Gap Between Models	Top-1	Top-2	Top-3	Top-4	Top-5
LiGAN to DecompDiff	0.31	0.61	0.77	0.81	0.85
DecompDiff to TargetDiff	0.50	0.32	0.18	0.09	0.04
TargetDiff to DrugGPS	4.17	4.37	4.46	4.54	4.61
DrugGPS to AR	-0.07	0.23	0.31	0.47	0.54
AR to FLAG	5.78	5.71	5.86	5.85	5.87
FLAG to Pocket2Mol	5.92	6.37	6.42	6.31	6.32

An analysis of Table 7 reveals a crucial insight: superior molecular properties do not necessarily translate to higher round-trip scores or search success rates. This observation underscores a critical aspect of molecular generation in drug discovery - the importance of balancing molecular quality with synthesizability. While generating high-quality molecules is essential, ensuring that these molecules are practically synthesizable is equally crucial for advancing potential drug candidates. This finding highlights the need for a holistic approach in generative models for drug discovery, one that considers both the desirable properties of molecules and their feasibility for synthesis.

Table 7: Comparing the generated molecules' properties by different generative models. We report the means and standard deviations. The properties of the test dataset for the best results are bolded.

Model	Vina Score (kcal/mol, ↓)	High Affinity(↑)	QED (↑)	SA (↑)	LogP	Lip. (↑)	Sim. Train (↓)	Div. (↑)
LiGAN	-6.03±1.89	0.19±0.26	0.37±0.27	0.62±0.20	-0.02±2.48	4.00±0.92	0.41±0.22	0.67±0.15
AR	-6.11±1.66	0.24±0.23	0.48±0.18	0.66±0.19	0.21±1.76	4.69±0.45	0.39±0.21	0.65±0.13
Pocket2Mol	-6.87±2.19	0.41±0.23	0.52±0.24	0.73±0.21	0.83±2.17	4.89±0.22	0.36±0.19	0.70±0.17
TargetDiff	-5.47	0.58	0.48	0.58	-	-	-	0.72
FLAG	-6.96±1.92	0.45±0.22	0.55±0.20	0.74±0.19	0.75±2.09	4.90±0.14	0.39±0.18	0.70±0.18
DecompDiff	-5.67	0.64	0.45	0.61	-	-	-	0.68
DrugGPS	-7.28±2.14	0.57±0.23	0.61±0.22	0.74±0.18	0.91±2.15	4.92±0.12	0.36±0.21	0.68±0.15